Knowledge-based Engineering and Sciences (2023), **4**, (3), 1–16
doi:10.51526/kbes.2023.4.3.1-16

RESEARCH PAPER

Real-time flood inundation monitoring in Capital of India using Google Earth Engine and Sentinel database

Biswarup Rana*

Department of Remote Sensing and GIS, Vidyasagar University, Midnapore, India
*Corresponding author. Email: biswaruprana2017@gmail.com

(Received 14 November 2023; revised 07 December 2023; accepted 12 December 2023; first published online 31 December 2023)

Abstract

This study focuses on researching flood inundation and vulnerable areas in Delhi NCT using Remote Sensing (RS) and GIS techniques during flood from July 8 to July 15, 2023, with the entire analysis conducted through satellite and cloud-based processing methods, specifically employing the Google Earth Engine (GEE). Leveraging high-temporal satellites that gather data enables the identification of flooded zones in real-time, during floods, and in the aftermath. Analyzing data collected at different stages of a flood provides valuable insights for pinpointing affected areas. Water naturally flows from high to low elevation areas, and based on elevation data, lowest elevation regions, particularly along the Yamuna riverbank under Delhi NCT, are highly susceptible to flooding, are considered flood-prone areas and flood water inundated. A thorough comprehension and flood-prone area mapping, along with a map illustrating highly inundated zones. After obtaining flood inundation maps and overlaying them with Land Use and Land Cover (LULC) classified maps, the study identified specific areas that experienced flood inundation. The analysis generated a flood zone map, indicating that the flooded area encompasses approximately 110 km², within a total study area of 1488.4 km². The affected areas have elevations ranging from 200 to 210 meters, whereas the maximum elevation in the study area is approximately 326 meters. The GEE platform is employed for processing, utilizing a Supervised classification algorithm for LULC mapping, and an Inverse Distance Weight method for mapping temperature and rainfall. This study utilized the GEE platform to create pre- and post-flood maps based on Sentinel 1 satellite datasets. Generated DEM, and employed it to create various surface estimation maps, including a stream order map. The GIS is employed to enhance the efficiency of monitoring and managing flood disasters, with the high temporal and spatial resolution data playing a pivotal role in flood monitoring.

Keywords: Flood inundation mapping; Sentinel 1/2; Climate analysis; Remote Sensing; Google Earth Engine.

1. Introduction

Flooding represents a widespread occurrence that presents a significant challenge for urban planners globally. Flooding happens rapidly due to the swift flow rates. In densely populated urban areas, inhabitants in vulnerable zones frequently face the threat of floods, impacting a range of properties, including commercial, industrial, agricultural, and institutional structures. These challenges occasionally lead to loss of life, underscoring the importance of resilience across social, economic, institutional, infrastructure, and community capital dimensions [1], [2].

Indian metropolitan cities such as Delhi, Mumbai, Pune, Ahmedabad, Surat, Chennai, Kolkata, Bangalore, and Hyderabad face severe flood inundation issues during heavy rainfall. The swift growth

of urban cities, coupled with industrial expansion and unplanned development, results in significant challenges when confronted with natural hazards or disasters. The examination of the flood zoning pattern indicates that high-risk zones are typically areas previously indicated the unstructured and unplanned areas [3]. That areas are characterized by isolated buildings and populations. The Yamuna River, a primary freshwater source for Delhi, has been adversely affected by the city's high-water demand and subsequent wastewater release [4]. The Yamuna River, special in heavy rainfall during monsoons has a destructive impact on the daily lives, and property, farmer, and municipality areas, especially those living in close to river banks [5]–[7]. Floods are immensely destructive phenomena intense of climate due to rapid urbanization and rainfall results in rapid runoff due to the reduction of water absorption caused by extensive concrete surfaces, land use patterns. This, in turn, hampers groundwater table recharge, public and private assets, local landscape, cattle and exacerbates drought-related issues etc [8]–[11] The connection between land use and flooding is complex; urbanization in catchment areas can potentially trigger floods, leading to substantial economic losses [12], [13]. Additionally, it is influenced by drainage basin conditions, including pre-existing water levels in rivers [14], [15]. The repercussions of floods extend beyond compromised land use, disrupting community life, damaging properties, and affecting road transport, agricultural, thereby disturbing the environmental sustainability [6], [16]–[19]. Every year, approximately 7.5 million hectares of land are impacted, causing damages worth Rs. 1805 crores to crops, houses and public utilities due to flooding and also an average of 140 million people affects annually (https://ndma.gov.in/). Rapidly growing / changing of land use pattern and environment, the inevitability of rising flood disaster underscores the crucial requirement for meticulous monitoring, assessment and delineation of highly vulnerable flood risk area to ensure effective flood mitigation in the future [20]–[22]. The extent of devastating urban floods depends on factors like heavy rainfall, flood depth, velocity, and duration. Urban flooding is a result of intense rainfall caused by impermeable surfaces and obstructed or insufficient sewage and drainage systems, consistently impacting the flow dynamics [23]–[27]. Additionally, rapid land use pattern change, causes significant sedimentation and solid water accumulation along riverbanks. This diminishes the river's water-carrying capacity, leading to increased flood susceptibility, in urban areas near rivers may experience overbank flow, exacerbated by excessive water loads, high tides at river mouths, and other contributing factors [28], [29]. In the past few decades, the use of remotely sensed imagery and GIS-based multi-criteria methods has proven highly effective in pinpointing real-time monitoring of the spatial aspects of floods, aiding in the identification of vulnerable areas for efficient flood management [30]–[34]. The role of Remote sensing earth observation data and GIS powerful tools, high-resolution satellite images, land use data, DEM elevation, slope, watershed, and drainage details are vital for flood hazard mapping, risk assessment, and monitoring. Determining flood depth, and structural measures relies on hydrological or remotely sensed data [35]–[39].

The novelty of the research is to find out the near real-time flood monitoring in the recent flood occurring in the Delhi NCR using Sentinel-1-based flood inundation in the GEE platform. Utilizing remote sensing and GIS techniques effectively enables us to discern alterations before and after disasters, assess temporal shifts, quantify the extent of devastation, and anticipate vulnerable areas for future occurrences.

2. Materials and Methods

2.1 Location map of the study area

The Delhi National Capital Territory (NCT) stands out as the primary commercial centre in northern India, functioning as a significant hub for small industries. Delhi is bordered by Haryana on all sides except the east, where it shares its border with Uttar Pradesh. Spanning an extensive area of 1489 square kilometres, Delhi NCT is located between latitudes 28°2401500 and 28°5300000 N, and longitudes 76°5002400 and 77°2003000 E, with an average elevation varying from 229

meters to 300 meters above sea level (https://delhi.gov.in/). According to the 2011 census, Delhi had an approximate population of 1.68 crores, with a population density of 11,320 people per square kilometre. Among this population, 24.90% resided in rural areas, while 75.10% lived in urban areas (https://delhiplanning.delhi.gov.in/planning/economic-survey-delhi-2022-23). As per the Meteorological Department, the region experiences a semi-arid climate marked by harsh summers and winters, with June being the hottest month and January the coldest (Metrological Department of Delhi). Delhi flood plain is divided into Flood plain with recent river deposits, Lower alluvial plain, and Upper alluvial plain (https://icar.org.in/). Regarding Delhi's land use pattern, the total land area covers 147,488 hectares, with approximately 70% being rural and 30% urban (https://delhiplanning.delhi.gov.in/). In terms of groundwater, it is relatively shallow (Fig 1). Within the Delhi NCT, natural vegetated areas consist of trees, herbs, and shrubs. Around 25% of the total irrigated area in Delhi receives water from three government canals: Western Yamuna Canal, Eastern Yamuna Canal, and Agra Canal. The combined length of these canals is approximately 56 km, with the majority of the canal-irrigated area being served by the Western Yamuna Canal. Yamuna, a notable tributary of the Ganga River, traverses Uttarakhand, Haryana, Delhi, and Uttar Pradesh. In Delhi, the river significantly diminishes, drying up in specific segments for around nine months annually. The stretch from Wazirabad to Okhla, spanning 22 km within Delhi, is particularly affected despite the river's total length of 54 km from Palla to Badarpur (https://environment.delhi.gov.in/). Delhi total 24,840 ha of floodplains and 68 % area under Yamuna River floodplains.

2.2 Dataset use and methodology

This study employs cloud-based remote sensing processing techniques, specifically utilizing GEE code editor for data download, processing, masking also for information extraction. This study utilized Sentinel-1 satellite data, specifically employing VV (Single co-polarization, vertical transmit/vertical receive) and VH (Dual-band cross-polarization, vertical transmit/horizontal receive) bands for mapping flood areas. Data collection occurred from July 8, 2023, to July 15, 2023, to detect the flood event, and pre-flood data was gathered between June 25, 2023, and June 4, 2023. For the LULC classification, the study employed a supervised image classification technique (Fig 2). This study utilized Sentinel-2 visual data with a resolution of 10 meters in the process. To enhance data visualization, a median filter and a 1% threshold for cloud cover pixel percentage were applied. Also, in this study used ALOS DEM to extract elevation and slope information within the study area. Furthermore, for delineating stream orders, this study employed the same ALOS DSM data within the GEE code editor. In this study, Google Earth Pro was to delineate the main river channel, major drains, and basin area. This study obtained 30s Temperature and 30s Precipitation data from the 'WorldClim' weather and climate information website (www.worldclim.org), which is akin to IMD climate data. To create specific map layouts, diagrams, and charts in this study, utilized ArcGIS software v10.8, QGIS, and Microsoft Excel software.

3. Modeling Results

In this study, maps illustrating the cumulative and temporal extent of LULC, Temperature, and Precipitation maps were generated [40], [41]. To assess surface characteristics, maps depicting Elevation, Slope, Contour, Stream Order, Aspect, and Hillside were generated. Subsequently, by compiling and illustrating all gathered information, a map delineating flood-inundated areas was created.

3.1 Elevation and Surface Estimation

Topography significantly influences flood severity, with direct effects on flow size and runoff velocity, crucial for identifying flood-prone areas [42]–[45]. Upon reviewing the results, it is evident that the downstream section of the Yamuna River catchment area is identified as the most significant

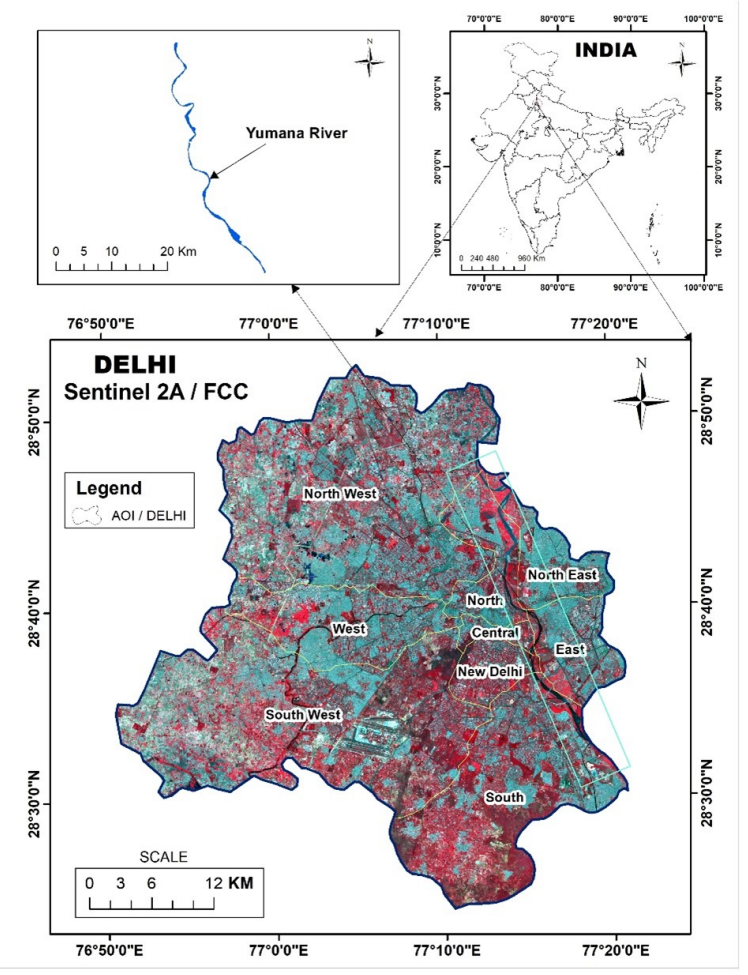

Figure 1: *Location map of the study area.*

vulnerable area, this area is characterized as a high-risk flood zone and this area under the lowest elevation. In this study, ALOS PALSAR DEM data was employed to represent elevation information. The highest elevation in Delhi NCT ranges from 267 to 326 m, with the overall terrain varying between 186 to 326 m above mean sea level. The catchment area of the Yamuna River under Delhi NCT ranges from 200 to 210 m (Fig 3). This study aims to develop a technique for simulating surface flow paths based on a digital elevation model. The Hillshade values range from 26 (minimum) to 251 (maximum), the Aspect map spans degrees from 1 (minimum) to 359 (maximum), and the slope map in the Delhi study area shows slopes ranging from 0 to 92 degrees. Furthermore, the contour level in this region extends from 180 meters (lowest) to 300 meters (highest) above mean sea level (AMSL). The stream order is divided into orders 1 to 4.

3.2 LULC

The frequency of flood occurrences is closely linked to changes in land-use patterns over time and their dynamic evolution and modifications [46]–[48]. This study used (GEE along with Sentinel-2 satellite data at a 10 m resolution visual band for the calculation and collection of LULC signatures

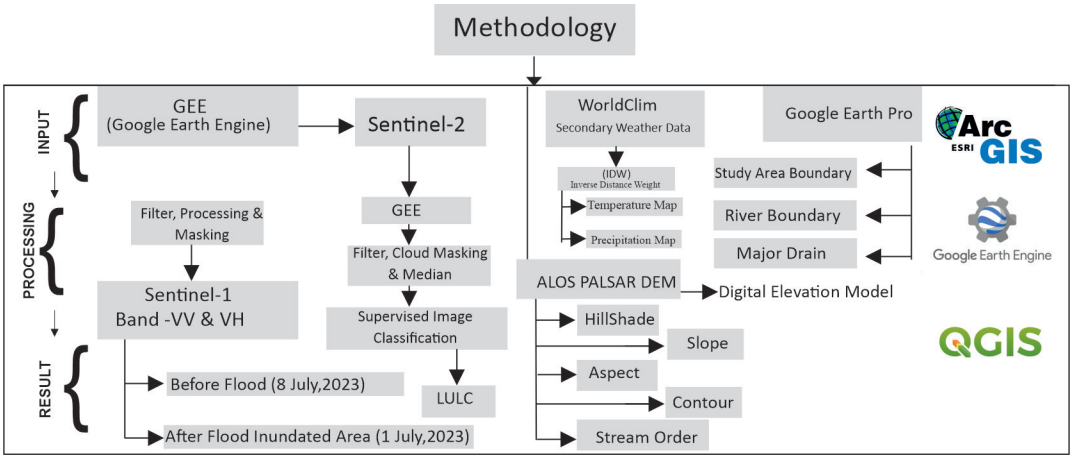

Figure 2: *Adopted methodology of the study area.*

(Fig 4). The area encompasses various LULC categories, including agricultural, Built-up, Open land, and Water bodies, as well as Vegetation. The analysis of LULC data reveals that Water bodies 58.85 km^2 (3.95%), Open land 341.89 km^2 (21.16%), Vegetation 242.6 km^2 (16.30%), Agricultural land 519.32 km^2 (34.89%) and Built Up area cover 352.74 km^2 (23.70%) area (Fig 5).

3.3 Temperature and Precipitation

The temperature changes play a significant role in altering rainfall patterns, and the disparity in extreme precipitation is almost linearly related to variation in temperature [49]. The rise in rainfall levels is leading to heightened flooding intensity [50]. The map displaying rainfall and temperature patterns was generated through the Inverse Distance Weight (IDW) method, integrating verified historical WorldClim climate data arranged in a gridded format (the 30s and 2.5m) (Fig 6). The research area's rainfall was categorized into five groups according to their impact on flood risk. Notably, the lowest category raged from 54-66 mm, while the highest category spanned from 62-63 mm. After computing the index, it was observed that the areas with the highest precipitation were notably in the northwest, north-central, east, and north-eastern parts of Delhi NCT (Fig 7). Conversely, the areas with the lowest precipitation were notably in the southwest, south, and certain parts of the northeast. The continuous rise in population due to rapid urbanization has led to escalating population and increasing temperatures in various areas. In Delhi NCT average temperature (30s) grided data, notable the highest temperature was 25 degrees Celsius. However, in the year 2021, Delhi NCT experienced significant temperature variation, with a notable maximum of 32.50 degree Celsius and a minimum of 19.10 degree Celsius at a height of 2.5m. Upon examining historical precipitation and temperature data, it is noteworthy that in 2010, the highest average precipitation was recorded at 70.99 mm, while in 2015, it was 53.60 mm, and in 2021, it reached 89.80 mm. Regarding temperatures, the highest average temperature in 2010 was 33.25°C, in 2015 it was 32.40°C, and in 2021, it was again notable at 32.25°C (Fig 8). It is worth mentioning that the southwestern and middle-western district portions of Delhi NCT consistently experienced the highest temperatures throughout these years.

3.4 Validation for flood inundation area

Typically, land bordering rivers has a gentle slope and vice versa, so even a slight rise in the river's water level can lead to flooding in these areas (Fig 9). Floods happen when land is submerged,

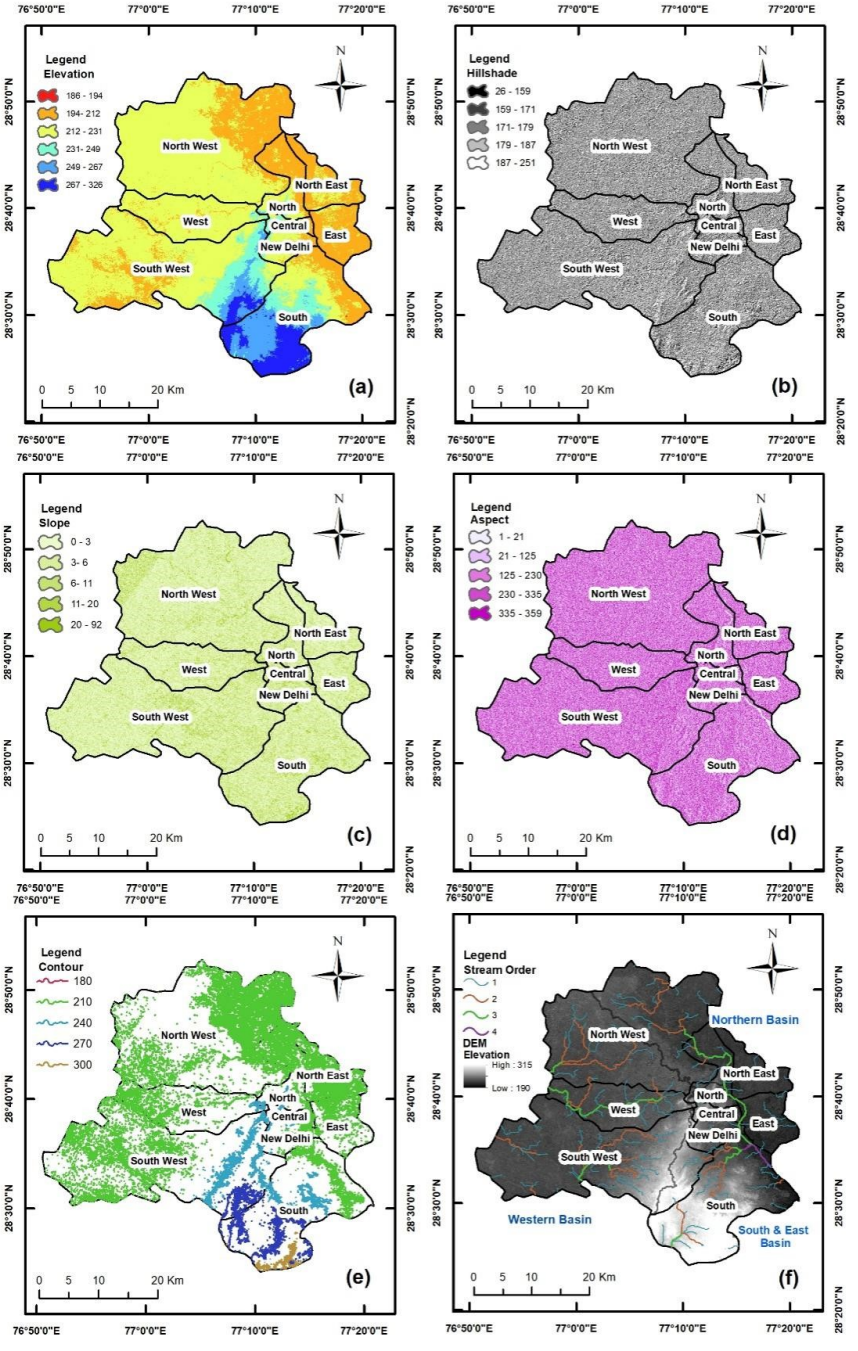

Figure 3: *Criteria of the selected study area.*

influenced by surface topography and lower elevations face increased flooding frequency, making them more vulnerable to inundation [51]. The study demonstrates the application of Remote Sensing and GIS techniques [52], utilizing Sentinel-1's VV and VH bands along with the GEE platform

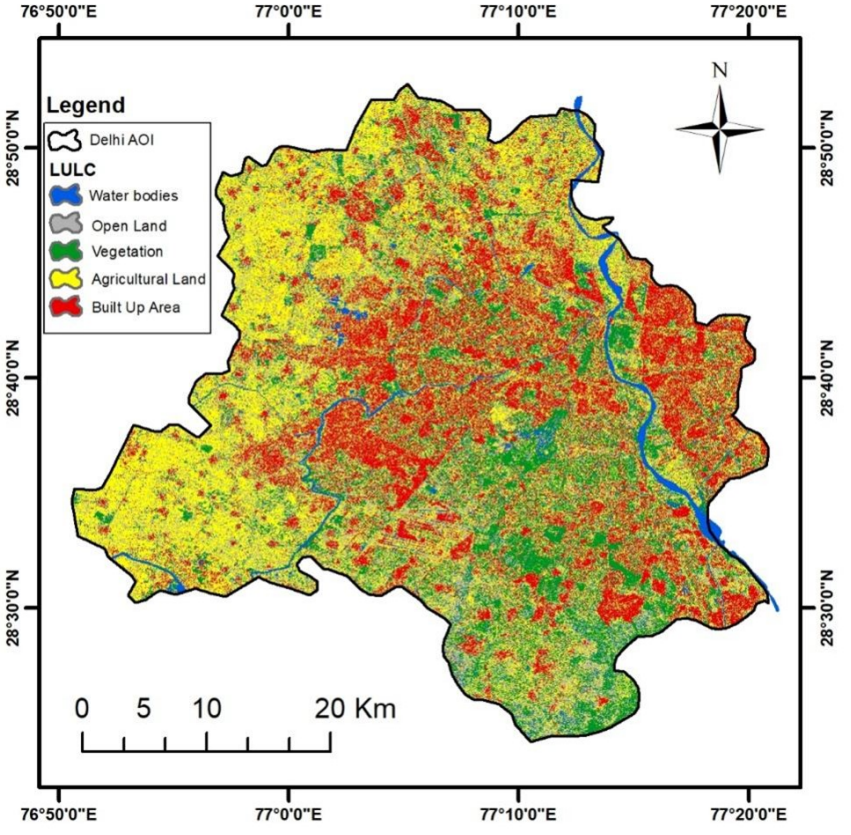

Figure 4: *Derived Spatio-temporal pattern LULC map over study area.*

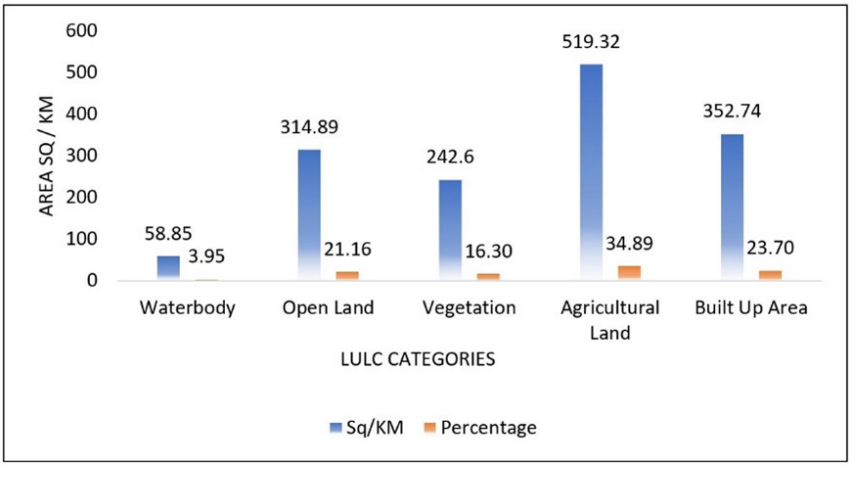

Figure 5: *Details about the LULC classes.*

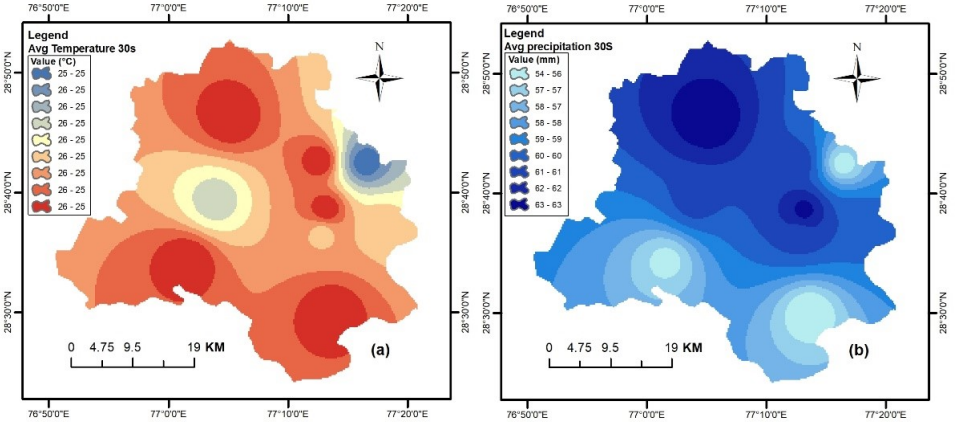

Figure 6: *Spatial variation of average Temperature and Precipitation (30s) Map of the study area. (a)Average Temperature, (b) Average Precipitation.*

[53], to accurately map flood-prone and inundated areas. The study primarily highlights that the riverbank areas of the Yamuna River in Delhi NCT are extensively inundated during floods and highly susceptible to flooding. After analyzing the data and performing calculations, it is evident that out of the total 1488.4 km2 area in Delhi NCT, 110 km2 is prone to flood inundation from July 8, 2023, to 15 July 2023. In this study, the prominently affected and flood-submerged area is the northeastern district portion of Delhi NCT. On both sides of the riverbank, an extensive area of over 3.5 km is significantly inundated by floods. The primary flood-prone area is situated along the banks of the Yamuna River, characterized by low elevation (201 m to 206 m). The urban developments in this region are highly vulnerable to flooding, particularly during the rainy season, leading to significant and destructive consequences (Fig 10). In these areas, floods disrupt roads, construction activities, metro services, and daily life. Once the floodwaters recede, significant soil erosion, damage to roads, and impact on private properties are observed. Additionally, during flood times, waterlogged areas are found in almost all districts of Delhi NCT, varying from place to place. The northeastern, eastern, and lower elevated southern regions of Delhi are particularly prone to flooding and inundation (Fig 11).

4. Limitations and Recommendations

The primary constraint in urban flood monitoring lies in real-time field data collection and preparation, which is essential for effective flood management. Real-time flood forecasting aims to mitigate the impact of floods and identify damages, especially in areas where physical presence is challenging. The main hurdles include the inability to access the location, limited data availability, and a crucial need for expertise in developing such systems. Timely acquisition of dynamic field data is crucial for making informed decisions and identifying optimal sites to mitigate disasters in vulnerable areas. Occasionally, satellite images may lack clarity due to cloudy and hazy weather conditions, and urban areas exhibit varying climatic conditions influenced by factors such as infrastructure and industrial development. As a result, weather conditions can rapidly shift across different areas. Significantly, this study utilized rapid temporal satellite data, elevation data, and statistical interpolation techniques to interpolate precipitation and temperature conditions in the study areas. Conducting a household survey during a flood is challenging, making it difficult to assess mental health issues at that time and to gather information on post-flood conditions, including the family's well-being, health, medical needs, access to food, transportation challenges, infrastructure issues, and property concerns in low-

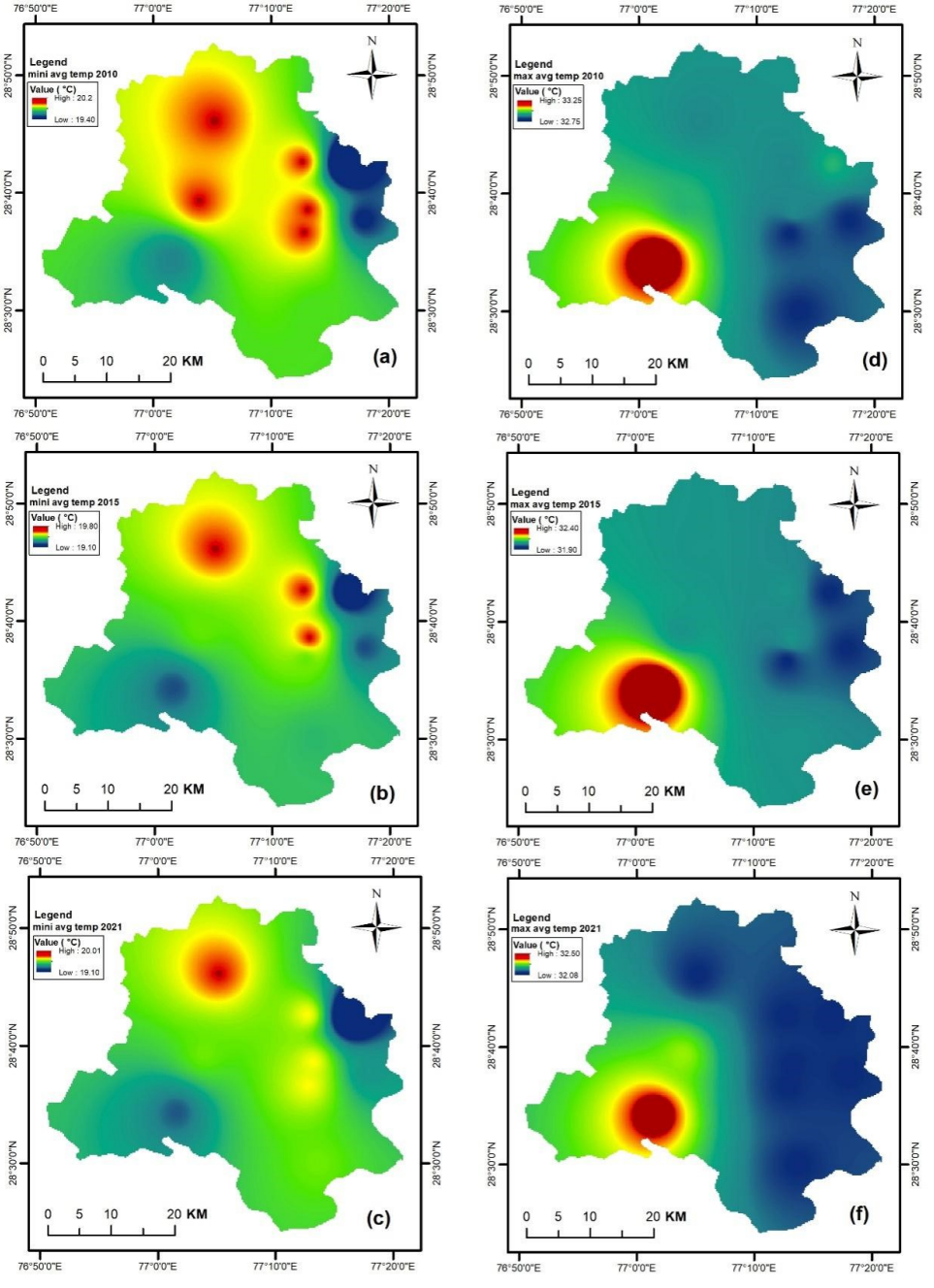

Figure 7: *Derived Spatial-temporal variation map of 2.5m average maximum and minimum Temperature (°C) from 2010 to 2021 in 5 years gap. (a)Minimum average temp of 2010, (b)Maximum average temp of 2010, (c) Minimum average temp of 2015, (d) Maximum average temp of 2015, (e) Minimum average temp of 2021, (f) Maximum average temp of 2021.*

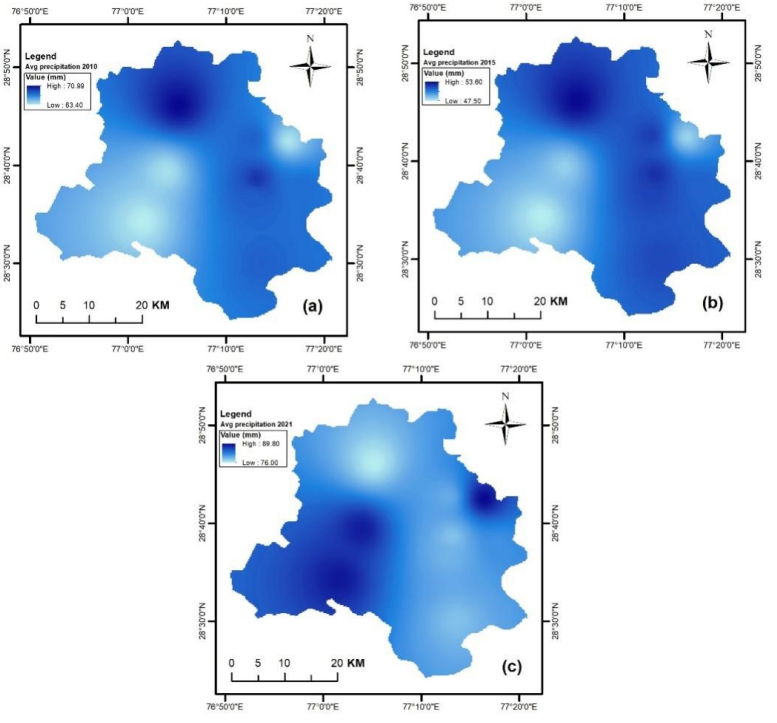

Figure 8: *Derived Spatial-temporal variation map of 2.5m average precipitation (mm) from 2010 to 2021 in 5 years gap. (a) Average precipitation map of 2010, (b) Average precipitation map of 2015, ©(a) Average precipitation map of 2021.*

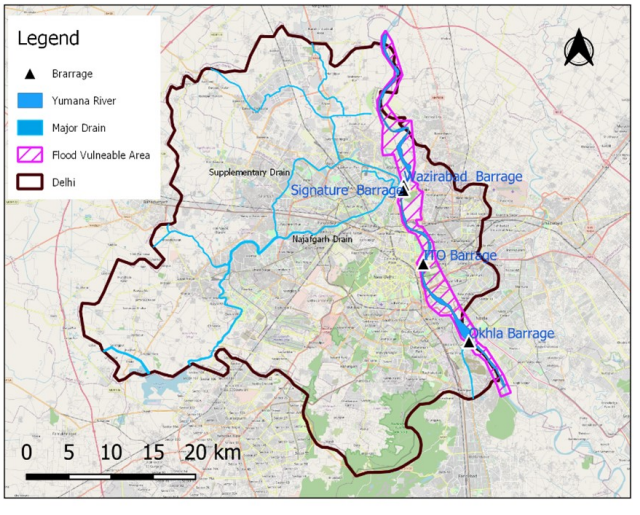

Figure 9: *Derived information map about major Drain, Barrage Flood Vulnerable areas.*

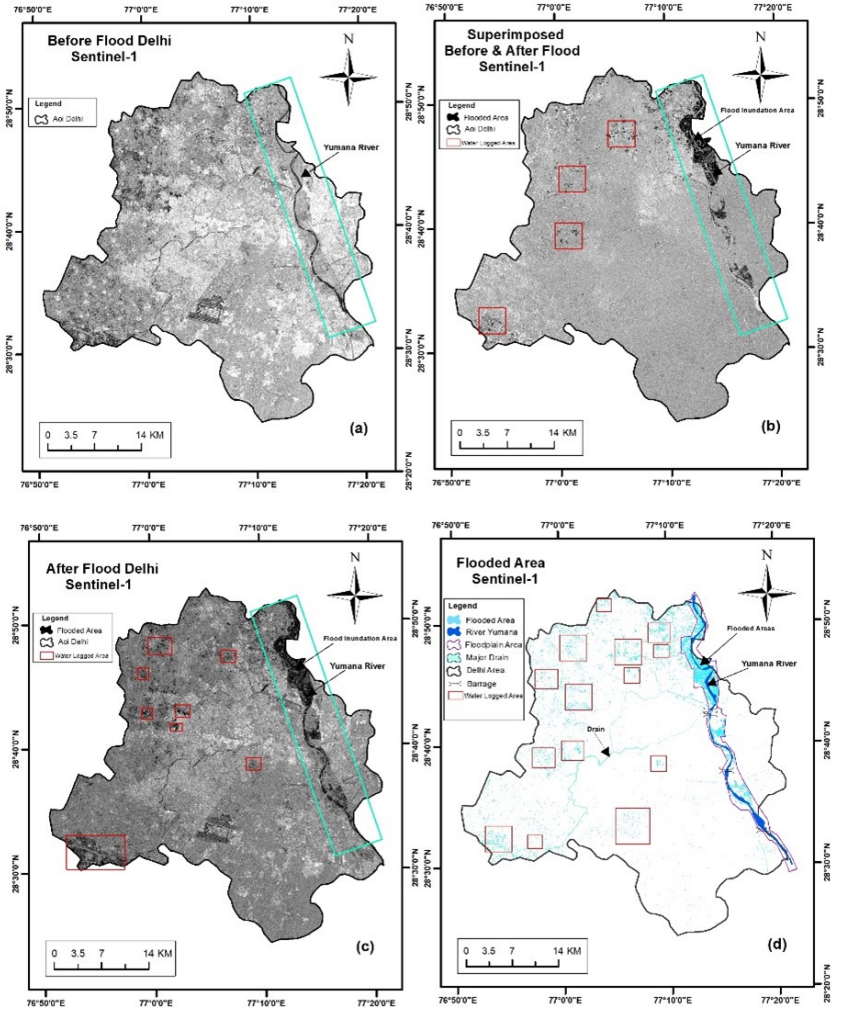

Figure 10: *Map depicting Flood Inundation area under Delhi NCT on July 8, 2023 in between July 15, 2023: (a) Before Flood in Delhi NCT, (b) Superimposed image of before and after flood in Delhi NCT, (c) After flood in Delhi NCT areas, with flood inundated areas and Water-logged areas (d) Capture Only flood inundated and water-logged areas.*

lying areas. This study leverages the GEE cloud platform to address data collection and assessment challenges. Urban areas are undergoing swift expansion, and alterations in land use, infrastructure, and climate contribute to evolving flood patterns over time. It is advisable for upcoming research to assess the extent of flood damage and employ monitoring techniques in flooded areas to identify key measures for mitigating future flood impacts. Daily life in urban areas encounters substantial disruptions caused by the catastrophic threat of floods, leading to a vulnerability in critical infrastructure like roads, bridges, and buildings, electricity, trade, telecommunication, etc. These components are frequently at risk of damage when confronted with flood-related challenges. Consequently,

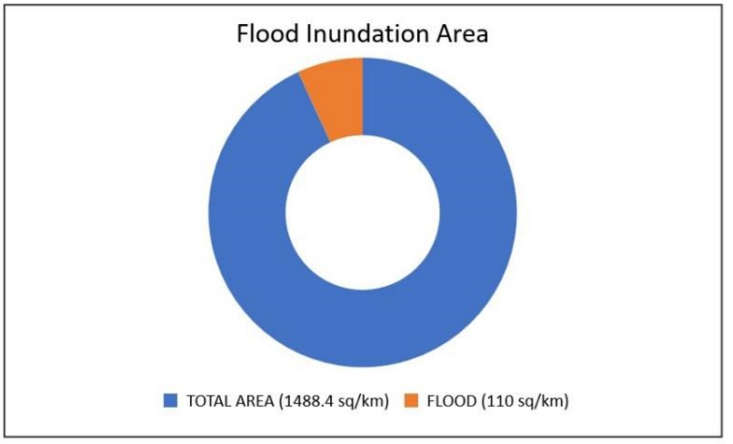

Figure 11: *Diagram showing amount Flood Inundation Area.*

roads become impassable, and large portions of the city quickly succumb to flooding. The SOP department of the Public Works Department (PWD) should oversee the maintenance of urban drains and canals ensuring they are clean and free from sedimentation. Moving forward, no areas must be developed without meticulous planning and lithological truthing to avoid potential issues. The Climate and Disaster Management Authority can leverage remote sensing and GIS techniques, along with advanced Hydraulic modeling and monitoring methods, to accurately assess affected areas and flood return period prediction. For swift disaster management and monitoring, the utilization of UAV (Unmanned aerial vehicle) and ML (Machine Learning) techniques is highly recommended.

5. Conclusions

This research introduces a novel approach focused on precisely delineating flood-inundated areas. The study utilizes multi-band, high spectral, and temporal resolution satellite data, employing the GEE cloud processing technique and error reduction algorithm to mitigate data noise. The method includes filtering and delineating pre- and post-flood inundated areas. The use of cloud processing facilitates obtaining accurate information swiftly, without bias and eliminates the need for field surveys. The comprehensive processing of flood-inundated zones involves utilizing Sentinel-1 VV and VH bands. The findings emphasize the heightened flood vulnerability of lower elevation areas, particularly noteworthy along the Yamuna River bank in the northeast and east-northwest districts of Delhi. Prominent flood-affected areas include Wazirabad, Rajghat Road, Panchayara (Uttar Pradesh), and various other waterlogged locations in Delhi. The Yamuna River banks' lower elevation areas are particularly susceptible to flooding during the rainy season due to sedimentation, resulting in a diminishing water-carrying capacity. This leads to rapid and effective backing up of the river, rendering the surrounding areas highly vulnerable to flooding. Additionally, upstream drainage systems tend to overflow their banks following heavy rainfall, contributing to the heightened flood risk in these regions. The adverse consequences of flooding encompass the loss of both private and government property, agricultural land, harm to farmers and the economy, and destruction of buildings, settlements, and shelters. Furthermore, there is a detrimental impact on the quality of raw water in flooded areas, particularly affecting drinking water sources.

Conflicts of Interest: **The authors declare no conflict of interest.**

References

[1] M. J. Hammond, A. S. Chen, S. Djordjević, D. Butler, and O. Mark, "Urban flood impact assessment: A state-of-the-art review," Urban Water J, vol. 12, no. 1, pp. 14–29, 2013, doi: 10.1080/1573062x.2013.857421.
[2] B. Halder and · Jatisankar Bandyopadhyay, "Monitoring the tropical cyclone 'Yass' and 'Amphan' affected flood inundation using Sentinel-1/2 data and Google Earth Engine", doi: 10.1007/s40808-022-01359-w.
[3] B. Halder, S. Das, J. Bandyopadhyay, and P. Banik, "The deadliest tropical cyclone 'Amphan': investigate the natural flood inundation over south 24 Parganas using google earth engine," Safety in Extreme Environments, pp. 1–11, 2021.
[4] S. K. Bhagat, T. M. Tung, and Z. M. Yaseen, "Development of artificial intelligence for modeling wastewater heavy metal removal: State of the art, application assessment and possible future research," J Clean Prod, vol. 250, p. 119473, 2020, doi: 10.1016/j.jclepro.2019.119473.
[5] J. Anand, A. K. Gosain, and R. Khosa, "Prediction of land use changes based on Land Change Modeler and attribution of changes in the water balance of Ganga basin to land use change using the SWAT model," Science of the total environment, vol. 644, pp. 503–519, 2018.
[6] P. Tomar et al., "GIS-Based Urban Flood Risk Assessment and Management—A Case Study of Delhi National Capital Territory (NCT), India," Sustainability, vol. 13, no. 22, p. 12850, 2021, doi: 10.3390/su132212850.
[7] Z. M. Yaseen and S. Shahid, "Drought Index Prediction Using Data Intelligent Analytic Models: A Review," in Intelligent Data Analytics for Decision-Support Systems in Hazard Mitigation, Springer, 2020, pp. 1–27.
[8] U. Pawar, W. Suppawimut, N. Muttil, and U. Rathnayake, "A GIS-Based Comparative Analysis of Frequency Ratio and Statistical Index Models for Flood Susceptibility Mapping in the Upper Krishna Basin, India," Water (Basel), vol. 14, no. 22, p. 3771, 2022, doi: 10.3390/w14223771.
[9] S. Cai, J. Fan, and W. Yang, "Flooding Risk Assessment and Analysis Based on GIS and the TFN-AHP Method: A Case Study of Chongqing, China," Atmosphere (Basel), vol. 12, no. 5, p. 623, 2021, doi: 10.3390/atmos12050623.
[10] P. . R. Dhumal, "Dynamic Wave Modeling and Flood Mapping For a Reach of Krishna River Using Spatial Techniques," Int J Res Appl Sci Eng Technol, vol. V, no. XI, pp. 2291–2296, 2017, doi: 10.22214/ijraset.2017.11322.
[11] N. M. Ogarekpe, E. A. Obio, I. T. Tenebe, P. C. Emenike, and C. C. Nnaji, "Flood vulnerability assessment of the upper Cross River basin using morphometric analysis," Geomatics, Natural Hazards and Risk, vol. 11, no. 1, pp. 1378–1403, 2020, doi: 10.1080/19475705.2020.1785954.
[12] B. Halder, T. Tiyasha, S. Shahid, and Z. M. Yaseen, "Delineation of urban expansion and drought-prone areas using vegetation conditions and other geospatial indices," Theor Appl Climatol, 2022, doi: 10.1007/S00704-022-04108-2.
[13] B. B. Ghute, M. B. Shaikh, and · Bijay Halder, "Modeling Earth Systems and Environment Impact assessment of natural and anthropogenic activities using remote sensing and GIS techniques in the Upper Purna River basin, Maharashtra, India," vol. 1, p. 3, doi: 10.1007/s40808-022-01576-3.
[14] Z. W. Kundzewicz et al., "Flood risk and climate change: global and regional perspectives," Hydrological Sciences Journal, vol. 59, no. 1, pp. 1–28, 2013, doi: 10.1080/02626667.2013.857411.
[15] B. Halder, "Investigation of the extreme weather conditions and anthropogenic activities in Island ecosystem," Safety in Extreme Environments, pp. 1–20, 2022.
[16] M. Masood and K. Takeuchi, "Assessment of flood hazard, vulnerability and risk of mid-eastern Dhaka using DEM and 1D hydrodynamic model," Natural Hazards, vol. 61, no. 2, pp.

757–770, 2011, doi: 10.1007/s11069-011-0060-x.
[17] A. Al Faisal, A. Al Kafy, and S. Roy, "Integration of Remote Sensing and GIS Techniques for Flood Monitoring and Damage Assessment: A Case Study of Naogaon District, Bangladesh," Journal of Remote Sensing amp; GIS, vol. 07, no. 02, 2018, doi: 10.4172/2469-4134.1000236.
[18] O. Singh and M. Kumar, "Flood occurrences, damages, and management challenges in India: a geographical perspective," Arabian Journal of Geosciences, vol. 10, no. 5, 2017, doi: 10.1007/s12517-017-2895-2.
[19] P. Brémond, F. Grelot, and A.-L. Agenais, "Review Article: Economic evaluation of flood damage to agriculture – review and analysis of existing methods," Natural Hazards and Earth System Sciences, vol. 13, no. 10, pp. 2493–2512, 2013, doi: 10.5194/nhess-13-2493-2013.
[20] I. O. RAUFU, I. MUKAİLA, K. OLANİYAN, and Z. AWODELE, "Application of Remote Sensing and Geographical Information System (GIS) in Flood Vulnerability Mapping: A Scenario of Akure South, Nigeria," International Journal of Environment and Geoinformatics, vol. 10, no. 1, pp. 90–99, 2023, doi: 10.30897/ijegeo.1073697.
[21] B. Halder, A. M. S. Ameen, J. Bandyopadhyay, K. M. Khedher, and Z. M. Yaseen, "The impact of climate change on land degradation along with shoreline migration in Ghoramara Island, India," Physics and Chemistry of the Earth, Parts A/B/C, vol. 126, p. 103135, 2022, doi: 10.1016/j.pce.2022.103135.
[22] B. Halder, A. Karimi, P. Mohammad, J. Bandyopadhyay, R. D. Brown, and Z. M. Yaseen, "Investigating the relationship between land alteration and the urban heat island of Seville city using multi-temporal Landsat data," Theor Appl Climatol, vol. 150, no. 1, pp. 613–635, 2022.
[23] Z. Zhu, Z. Chen, X. Chen, and P. He, "Approach for evaluating inundation risks in urban drainage systems," Science of The Total Environment, vol. 553, pp. 1–12, 2016, doi: 10.1016/j.scitotenv.2016.02.025.
[24] R. Ghorbani Kalkhajeh and A. A. Jamali, "Analysis and predicting the trend of land use/cover changes using neural network and systematic points statistical analysis (SPSA)," Journal of the Indian Society of Remote Sensing, vol. 47, no. 9, pp. 1471–1485, 2019.
[25] B. Liu et al., "Flooding by High-Concentration Polymer Doubled Oil Recovery of Common Polymer on Field Test with 20% Closed to the Result of Laboratory Test in Daqing," All Days. SPE, 2007. doi: 10.2118/108684-ms.
[26] J. Chen, A. A. Hill, and L. D. Urbano, "A GIS-based model for urban flood inundation," J Hydrol (Amst), vol. 373, no. 1–2, pp. 184–192, 2009, doi: 10.1016/j.jhydrol.2009.04.021.
[27] V. A. Rangari, N. V Umamahesh, and A. K. Patel, "Flood-hazard risk classification and mapping for urban catchment under different climate change scenarios: A case study of Hyderabad city," Urban Clim, vol. 36, p. 100793, 2021, doi: 10.1016/j.uclim.2021.100793.
[28] T. Tingsanchali, "Urban flood disaster management," Procedia Eng, vol. 32, pp. 25–37, 2012, doi: 10.1016/j.proeng.2012.01.1233.
[29] M. G. Macklin and J. Lewin, "River sediments, great floods and centennial-scale Holocene climate change," J Quat Sci, vol. 18, no. 2, pp. 101–105, 2003, doi: 10.1002/jqs.751.
[30] G. S. Ogato, A. Bantider, K. Abebe, and D. Geneletti, "Geographic information system (GIS)-Based multicriteria analysis of flooding hazard and risk in Ambo Town and its watershed, West shoa zone, oromia regional State, Ethiopia," J Hydrol Reg Stud, vol. 27, p. 100659, 2020, doi: 10.1016/j.ejrh.2019.100659.
[31] M. Singha et al., "Identifying floods and flood-affected paddy rice fields in Bangladesh based on Sentinel-1 imagery and Google Earth Engine," ISPRS Journal of Photogrammetry and Remote Sensing, vol. 166, pp. 278–293, 2020.
[32] K.-J. Douben, "Characteristics of river floods and flooding: a global overview, 1985–2003," Irrigation and Drainage, vol. 55, no. S1, pp. S9–S21, 2006, doi: 10.1002/ird.239.
[33] A. A. Memon, S. Muhammad, S. Rahman, and M. Haq, "Flood monitoring and damage

assessment using water indices: A case study of Pakistan flood-2012," The Egyptian Journal of Remote Sensing and Space Science, vol. 18, no. 1, pp. 99–106, 2015.
[34] P. Tomar et al., "GIS-Based Urban Flood Risk Assessment and Management—A Case Study of Delhi National Capital Territory (NCT), India," Sustainability, vol. 13, no. 22, p. 12850, 2021, doi: 10.3390/su132212850.
[35] J. Sanyal and X. X. Lu, "Application of Remote Sensing in Flood Management with Special Reference to Monsoon Asia: A Review," Natural Hazards, vol. 33, no. 2, pp. 283–301, 2004, doi: 10.1023/b:nhaz.0000037035.65105.95.
[36] S. Hammami et al., "Application of the GIS based multi-criteria decision analysis and analytical hierarchy process (AHP) in the flood susceptibility mapping (Tunisia)," Arabian Journal of Geosciences, vol. 12, no. 21, pp. 1–16, 2019.
[37] H. Mojaddadi, B. Pradhan, H. Nampak, N. Ahmad, and A. H. bin Ghazali, "Ensemble machine-learning-based geospatial approach for flood risk assessment using multi-sensor remote-sensing data and GIS," Geomatics, Natural Hazards and Risk, vol. 8, no. 2, pp. 1080–1102, 2017, doi: 10.1080/19475705.2017.1294113.
[38] Y. Wang, Z. Li, Z. Tang, and G. Zeng, "A GIS-Based Spatial Multi-Criteria Approach for Flood Risk Assessment in the Dongting Lake Region, Hunan, Central China," Water Resources Management, vol. 25, no. 13, pp. 3465–3484, 2011, doi: 10.1007/s11269-011-9866-2.
[39] H. Mojaddadi, B. Pradhan, H. Nampak, N. Ahmad, and A. H. bin Ghazali, "Ensemble machine-learning-based geospatial approach for flood risk assessment using multi-sensor remote-sensing data and GIS," Geomatics, Natural Hazards and Risk, vol. 8, no. 2, pp. 1080–1102, 2017, doi: 10.1080/19475705.2017.1294113.
[40] S. Mollah, "Assessment of Flood Vulnerability at Village Level for Kandi Block of Murshidabad District, West Bengal," Curr Sci, vol. 110, no. 1, p. 81, 2016, doi: 10.18520/cs/v110/i1/81-98.
[41] S. Mollah, "Assessment of Flood Vulnerability at Village Level for Kandi Block of Murshidabad District, West Bengal," Curr Sci, vol. 110, no. 1, p. 81, 2016, doi: 10.18520/cs/v110/i1/81-98.
[42] I. Pal, S. Singh, and A. Walia, "Flood management in Assam, INDIA: a review of brahmaputra floods, 2012," Int J Sci Res Publ, vol. 3, no. 10, p. 1, 2013.
[43] G. Di Baldassarre, G. Schumann, P. D. Bates, J. E. Freer, and K. J. Beven, "Flood-plain mapping: a critical discussion of deterministic and probabilistic approaches," Hydrological Sciences Journal, vol. 55, no. 3, pp. 364–376, 2010, doi: 10.1080/02626661003683389.
[44] H. Karahan, G. Gurarslan, and Z. W. Geem, "Parameter Estimation of the Nonlinear Muskingum Flood-Routing Model Using a Hybrid Harmony Search Algorithm," J Hydrol Eng, vol. 18, no. 3, pp. 352–360, 2013, doi: 10.1061/(ASCE)HE.1943-5584.0000608.
[45] R. Few, "Flooding, vulnerability and coping strategies: local responses to a global threat," Progress in Development Studies, vol. 3, no. 1, pp. 43–58, 2003, doi: 10.1191/1464993403ps049ra.
[46] S. Sugianto, A. Deli, E. Miswar, M. Rusdi, and M. Irham, "The Effect of Land Use and Land Cover Changes on Flood Occurrence in Teunom Watershed, Aceh Jaya," Land (Basel), vol. 11, no. 8, p. 1271, 2022, doi: 10.3390/land11081271.
[47] G. Benito, M. Rico, Y. Sánchez-Moya, A. Sopeña, V. R. Thorndycraft, and M. Barriendos, "The impact of late Holocene climatic variability and land use change on the flood hydrology of the Guadalentín River, southeast Spain," Glob Planet Change, vol. 70, no. 1–4, pp. 53–63, 2010, doi: 10.1016/j.gloplacha.2009.11.007.
[48] A. Panahi, B. Alijani, and H. Mohammadi, "The Effect of the Land Use/Cover Changes on the Floods of the Madarsu Basin of Northeastern Iran," J Water Resour Prot, vol. 02, no. 04, pp. 373–379, 2010, doi: 10.4236/jwarp.2010.24043.
[49] A. Mishra and S. C. Liu, "Changes in precipitation pattern and risk of drought over India in the context of global warming," Journal of Geophysical Research: Atmospheres, vol. 119, no. 13, pp. 7833–7841, 2014, doi: 10.1002/2014jd021471.

[50] K. Breinl, D. Lun, H. Müller-Thomy, and G. Blöschl, "Understanding the relationship between rainfall and flood probabilities through combined intensity-duration-frequency analysis," J Hydrol (Amst), vol. 602, p. 126759, 2021, doi: 10.1016/j.jhydrol.2021.126759.
[51] T. Thi An et al., "Flood vulnerability assessment at the local scale using remote sensing and GIS techniques: a case study in Da Nang City, Vietnam," Journal of Water and Climate Change, vol. 13, no. 9, pp. 3217–3238, 2022, doi: 10.2166/wcc.2022.029.
[52] B. Halder, J. Bandyopadhyay, K. M. Khedher, C. M. Fai, F. Tangang, and Z. M. Yaseen, "Delineation of urban expansion influences urban heat islands and natural environment using remote sensing and GIS-based in industrial area," Environmental Science and Pollution Research, pp. 1–24, 2022.
[53] B. Halder et al., "Machine learning based country level annual air pollutants exploration using Sentinel 5P and Google Earth Engine," Sci Rep, pp. 1–19, 2023, doi: 10.1038/s41598-023-34774-9.